GENERALIZATION OF THE FEIGENBAUM-KADANOFF-SHENKER RENORMALIZATION AND CRITICAL PHENOMENA ASSOCIATED WITH THE GOLDEN MEAN QUASIPERIODICITY

S. P. KUZNETSOV
Saratov Division of Institute of Radio-Engineering and Electronics, Russian Academy of Sciences, Zelenaya 38, Saratov, 410019, Russia

Abstract

The paper presents a two-dimensional version of the Feigenbaum-Kadanoff-Shenker renormalization group equation. Several universality classes of critical behavior are discussed, which may occur at the onset of chaotic or strange nonchaotic attractors via quasiperiodicity at the golden-mean frequency ratio. Parameter space arrangement and respective scaling properties are discussed and illustrated.

1. Introduction

In modern nonlinear dynamics the concept of synchronization is considered not only in a classic sense, as a periodicity in a motion of a self-oscillator induced by the driven force, but relates to a variety of situations when dynamics of autonomous systems or external force are chaotic, quasiperiodic etc. It is used to speak of synchronization in a generalized sense if the system reproduces some definite features of the time-dependence of the external force in its dynamics. (See [1] and references therein.)

In a context of multi-parameter analysis, domains of synchronization, as well as the bifurcation sets, may be thought geometrically, as some configurations in parameter space. To understand the parameter space structure, it is essential to reveal critical situations responsible for formation or destruction of synchronized and non-synchronized regimes, in particular, those associated with birth of chaos or strange nonchaotic attractors (SNA)

[2,3,4]. Apparently, as a rule, the critical situations allow analysis in terms of renormalization group (RG) approach, analogous to that developed by Feigenbaum for the period-doubling transition to chaos [5,6], and they are characterized by properties of universality and scaling specific to each type of criticality. The critical situations are classified naturally in order of their codimension, which is a minimal number of parameters to be adjusted to reach a critical situation under study.

One of the models traditionally used for analysis of synchronization and desynchronization is the classic circle map

$$x_{n+1} = x_n + r + (K/2\pi)\sin 2\pi x_n. \tag{1}$$

In the parameter plane of this map (r, K) a set of synchronization regions – Arnold tongues is present, and they approach the axis K=0 by their sharp edges at rational points of r. On the line K=1 a critical point exists that corresponds to destruction of quasiperiodic regime with the golden-mean rotation number $w = \lim x_n = (\sqrt{5}-1)/2$. Fine structure of the synchronization tongues and quasiperiodic regions near this point obeys universality and scaling properties deduced from the RG analysis of Feigenbaum, Kadanoff, Shenker [7], and Rand, Ostlund, Satija, Siggia [8,9]. We will refer to it as the *GM critical point* (GM stands for the 'golden-mean').

In the present paper we consider and discuss a generalized RG approach, which includes the critical behavior of GM type as a particular case. It opens a possibility to reveal and study new universality and scaling classes linked with a birth of SNA in quasiperiodically forced systems at the golden-mean frequency ratio. The approach is based on the two-dimensional version of the Feigenbaum-Kadanoff-Shenker equation.

In Sec. 2 the procedure of RG analysis appropriate for the golden-mean quasiperiodicity is explained, and a two-dimensional generalization of the approach of Feigenbaum-Kadanoff-Shenker [7] and Ostlund et al. [8,9] is developed. In Sec. 3 we discuss model systems including quasiperiodically driven logistic, circle, and fractional-linear maps. In Sec. 4 our generalized RG scheme is used to reproduce some results of classic analysis of quasiperiodic transition to chaos in the circle map. In Sections 5, 6, and 7 we review three novel types of critical behavior discovered in a course of joint research program with the group of nonlinear dynamics and statistical physics from Potsdam University (A. Pikovsky, U. Feudel, E. Neumann) [10,11,12]. For each type of criticality we illustrate scaling for the critical attractor associated with dynamics exactly at the critical point, and scaling of topography of the parameter plane near the criticality.

2. Two-dimensional generalization of the Feigenbaim-Kadanoff-Shenker equation

Let us consider quasiperiodic dynamics in some system with two basic frequencies, ω_1 and ω_2, and assume that two subsystems associated with these frequencies are coupled unidirectionally. To describe dynamics in terms of Poincaré map, we perform stroboscopic cross-section of the extended phase space by planes of constant time, separated by $T = 2\pi/\omega_2$. The first subsystem ("master") is independent of the second one, and the associated dynamical variable is the phase φ governed by equation $\varphi_{n+1} = \varphi_n + \omega_1 T \pmod{2\pi}$. For the second subsystem ("slave") we assume that the dynamics is essentially one-dimensional: $x_{n+1} = F(x_n, \varphi_n)$. In respect to the second argument the function $F(x, \varphi)$ is 2π-periodic. Instead of φ we introduce a variable u defined modulo 1:

$$x_{n+1} = f(x_n, u_n), \quad u_{n+1} = u_n + w \pmod{1}, \tag{2}$$

where $f(x, u) = F(x, 2\pi u)$, $w = \omega_1 T/2\pi = \omega_1/\omega_2$. In the further study we fix $w = (\sqrt{5} - 1)/2$.

In general context of nonlinear dynamics, the basic idea of the RG analysis consists in the following. We start with an evolution operator of a system on a definite time interval and apply this operator several times to construct the evolution operator for larger interval. Then, we try to adjust parameters of the original system to make the new operator reducible to the old one by scale change of dynamical variables. This procedure is called the RG transformation. The adjusted parameters will define location of the critical point. The RG transformation may be applied again and again to obtain a sequence of the evolution operators for larger and larger time intervals.

If the approach works, one possibility is that the produced operators become asymptotically identical, and we speak about a fixed point of the RG transformation. Another possibility is that they repeat each other after several steps of the RG transformation, and we speak about a periodic orbit, or a cycle of the RG equation. In any of these cases, the rescaled long-time evolution operators will be determined by structure of the RG transformation, rather than by concrete dynamical equations of the original dynamical system. This implies *universality*. On the other hand, repetition of the rescaled evolution operators at subsequent steps of the RG transformation means that the system manifests similar dynamics on different time scales. This implies *scaling*.

How can we apply this approach to critical phenomena associated with the golden-mean quasiperiodicity? As known, the convergent sequence of rationals for $w = (\sqrt{5} - 1)/2$ is defined as F_{k-1}/F_k, F_k are the Fibonacci

numbers: $F_0 = 0, F_1 = 1, F_{k+1} = F_k + F_k$. This sequence delivers the best possible approximation for w, so, the dynamics on a time interval F_k is close to periodic. Hence, it is natural to consider a sequence of evolution operators over intervals of discrete time given by the Fibonacci numbers.

Let $f^{F_k}(x,u)$ and $f^{F_{k+1}}(x,u)$ designate transformation of x after F_k and F_{k+1} iterations, respectively. To construct the next operator, for F_{k+2} iterations, we start from (x,u) and perform first F_{k+1} iterations to arrive at $(f^{F_{k+1}}(x,u),\ \ u+F_{k+1}w)$, and then the rest F_k iterations with the result

$$f^{F_{k+2}}(x,u) = f^{F_k}(f^{F_{k+1}}(x,u),\ u + wF_{k+1}). \tag{3}$$

To have a reasonable limit behavior of the evolution operators we change scales for x and u by some factors α and β at each new step of the construction, and define the renormalized functions as

$$g_k(x,u) = \alpha^k f(x/\alpha^k,\ u/\beta^k). \tag{4}$$

Note that $wF_{k+1} = -(-w)^{k+1} \pmod 1$, so it is natural to set $\beta = -1/w = -1.618034....$ Rewriting (3) in terms of the renormalized functions we come to the functional equation

$$g_{k+2}(x,u) = \alpha^2 g_k(\alpha^{-1} g_{k+1}(x/\alpha, -uw), w^2 u + w). \tag{5}$$

In the present article we deal with several different solutions of this equation – fixed points or cycles in the functional space. The constant α is specific for each universality class; it is evaluated in a course of solution of the functional equation.

The next step of the RG analysis consists in the following. Let us suppose that we deal now with dynamics in a vicinity of the critical point it in the parameter space. Then, a perturbation of the solution appears. Analyzing evolution of the perturbation of the evolution operators under subsequent application of the RG transformation we come to an eigenvalue problem. A number of relevant eigenvalues define a *codimension* of the critical situation. The relevant eigenvalues are those, which are larger than 1 in modulus, are not associated with infinitesimal variable changes, and do not violate the commutative properties of successively applied evolution operators (see e.g. [7-12] for some details). The codimension may be understood as a number of parameters, which must be adjusted to reach the criticality. For instance, in three-dimensional parameter space the codimension-one situations may occur at some surfaces, codimension-two situations at curves, and codimension-three at some points.

To derive an explicit form of the linearized RG equation appropriate for a vicinity of a fixed point $g(x,u)$ we substitute $g_k(x,u) = g(x,u) + \varepsilon h_k(x,u)$, $\varepsilon << 1$ and account terms of the first order in ε in Eq.(5). Then, setting

$h_k(x) = \delta^k h(x)$ we arrive to the eigenvalue problem

$$\delta^2 h(x,u) = \alpha\delta g'(g(x/\alpha, -uw), w^2u+w)h(x/\alpha, -uw)+\alpha^2 h(\alpha^{-1}g(x/\alpha, -uw),\ w^2u+w). \tag{6}$$

For each particular type of criticality, with specific $g(x,u)$ and α, this equation can be solved numerically to obtain spectrum of relevant δ.

3. Basic models

The simplest example, for which the developed RG scheme is applicable, is the well-known circle map (1). Figure 1 shows a chart of dynamical regimes

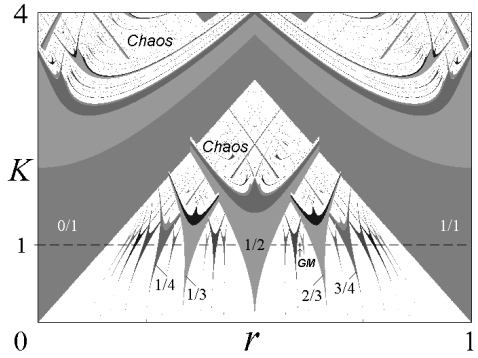

Figure 1. Chart of dynamical regimes on the parameter plane of the circle map. Numbers inside Arnold tongues indicate the respective rotation numbers.

on the parameter plane (r, K). For $K < 1$ one can observe periodic or quasiperiodic regimes associated with rational or irrational values of the rotation number defined as $\rho(r,K) = \lim_{n\to\infty} x_n/n$. Periodic regimes take place inside the Arnold tongues, and quasiperiodic motions are observed between of them. One can find a curve of constant golden-mean rotation number: $\rho(r,K) = w$. This curve starts at $K = 0$, $r = w$, and meets the critical line $K = 1$ at the GM critical point

$$K_{GM} = 1, r_{GM} = 0.60666106347\ldots \tag{7}$$

discovered by Shenker [13] and afterwards studied in terms of RG analysis by Feigenbaum–Kadanoff–Shenker and by Ostlund et al. [7-9].

Further examples of types of critical behavior discussed in the present article occur in quasiperiodically forced maps.

One model is the quasiperiodically driven logistic map [14-18, 10, 11]. A usual logistic map $x_{n+1} = \lambda - x_n^2$ is a basic model to study period-doubling transition to chaos. As it has the only relevant parameter λ, a natural generalization for presence of the external driving is to assume that this

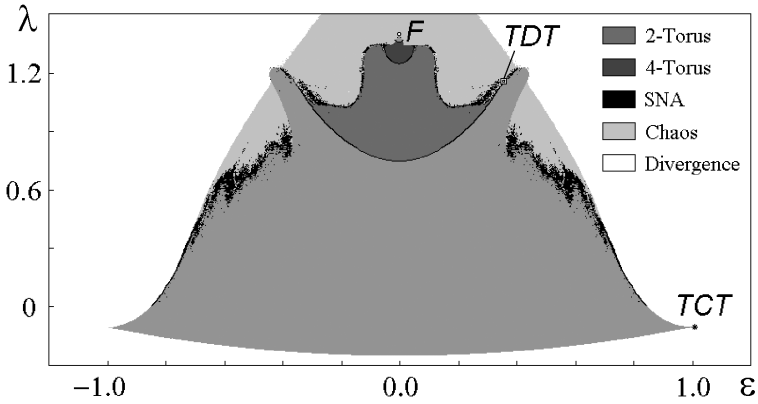

Figure 2. Chart of dynamical regimes on the parameter plane of quasiperiodically driven logistic map (8).

parameter is modulated with some frequency. In our study this frequency, measured in units of time discretization, is fixed, $w = (\sqrt{5}-1)/2$. So, the model is

$$x_{n+1} = \lambda - x_n^2 + \varepsilon \cos 2\pi n w. \tag{8}$$

Figure 2 shows a chart of dynamical regimes for this model on the parameter plane (ε, λ).

For $\varepsilon = 0$ Eq.(8) becomes the conventional logistic map. So, what is observed along the line $\varepsilon = 0$ is the usual period-doubling cascade, accumulated to the limit critical point of Feigenbaum (point F) [5,6,31].

First, let us take a value of λ at which the unforced map has a stable fixed point. At nonzero ε the fixed point will be transformed into a stable smooth invariant curve. In continuous-time dynamical systems such curves appear in the Poincaré cross-section for the motion on tori, so, with commonly used abuse of the terminology, we speak about the torus-attractor T1.

If the external force of small amplitude drives a stable period-2 orbit, it gives rise to an attractor consisting of two closed smooth curves, the doubled torus T2. Period-4 orbit generates, respectively, a four-piece invariant curve (torus T4), and so forth. In contrast to usual period-doubling, the sequency of torus-doubling transitions appears to be finite: the smaller amplitude of driving, the larger number of torus doublings seen in a course of increase of λ [14-20].

If we keep λ constant and increase the force amplitude, the smooth torus may transform into SNA: the Lyapunov exponent remains negative, but the geometrical structure of the attractor becomes complex, fractal-like. Also regimes with positive Lyapunov exponent arise for larger λ and

ε. With further increase of the parameters the orbits escape to infinity (white domain in Fig. 2).

As known, the parameter interval corresponding to existence of an attractive fixed point in the unforced logistic map $\lambda \in (-0.25, 0.75)$ is bounded on one side by the tangent bifurcation, collision of a pair of fixed points (stable and unstable), with their subsequent disappearance. On the other side it is bounded by the period-doubling bifurcation. Analogously, the bottom border of the domain T1 in Fig. 2 is the bifurcation curve of tori collision: attractor and repeller, represented by two invariant curves, approach each other, collide, and disappear. The top border is the bifurcation curve of torus doubling: the attractor originates here consisting of two closely placed curves, and after the bifurcation they move one off another.

Let us start at $\varepsilon = 0$, $\lambda = -0.25$ and increase ε to go in the parameter plane along the torus collision bifurcation curve. The situation of collision of smooth invariant curves takes place while the motion is confined on one side of the logistic parabola. At some value of ε the invariant curve at the bifurcation threshold touches the extremum $x = 0$. In accordance with argumentation of Ref.[11], it corresponds to the terminal point of the bifurcation line. This is a critical situation of particular interest, the *TCT critical point* (TCT stands for 'torus collision terminal') [11]:

$$\lambda_{TCT} = -0.09977122895\ldots, \varepsilon_{TCT} = 1.01105609099\ldots. \qquad (9)$$

Now, let us start at $\varepsilon = 0$, $\lambda = 0.75$ and move along the torus-doubling bifurcation curve. As in the previous case, this bifurcation of smooth invariant curve takes place only while the whole curve is placed on one side of the logistic parabola. At some value of ε the invariant curve at the bifurcation threshold touches the extremum $x = 0$, and the torus-doubling bifurcation line is terminated. This is the *TDT critical point* (TDT stands for 'torus-doubling terminal') [10]:

$$\lambda_{TDT} = 1.158096856726\ldots, \quad \varepsilon_{TDT} = 0.360248020507\ldots. \qquad (10)$$

TCT and TDT critical points were found also in quasiperiodically forced circle map

$$x_{n+1} = x_n + r - (K/2\pi)\sin 2\pi x_n + \varepsilon\cos 2\pi n w \pmod 1 \qquad (11)$$

in the supercritical case $K > 1$ (near the extrema it looks locally like the logistic map). In some respects, this is a more convenient object for detailed study: no divergence can occur in this map because the variable x is defined modulo 1.

Figure 3 shows a chart of dynamical regimes for the driven circle map on a part of the parameter plane (b, ε) including the TCT critical point [11].

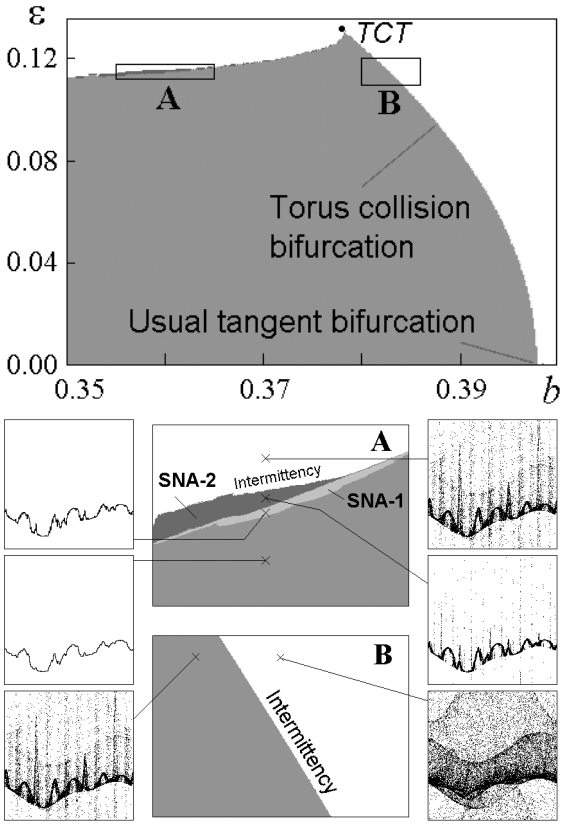

Figure 3. Chart of dynamical regimes on the parameter plane (b, ε) and two enlarged fragments with phase portraits of attractors on phase plane (u, x) at representative points.

Separately, two rectangular fragments of the chart are shown, together with phase portraits of attractors at representative points.

The large gray domain in the diagram corresponds to existence of the localized torus attractor. The right border of this domain is the bifurcation curve of bifurcation of collision of a pair of smooth tori, one stable and another unstable. After the event, both of them disappear, and intermittent regime occurs, with long-time travel of the orbits through the region of former existence of the tori (the 'channel'). Going along the bifurcation curve we observe that the semi-attractive invariant curve, formed at the moment of the collision, grows in size, and ultimately touches the minimum of the map; there we arrive at the TCT point. As found numerically, it is located at

$$r_{TCT} = 0.377866239..., \ \varepsilon_{TCT} = 0.132566321... \tag{12}$$

Another, upper border of the gray area corresponds to a situation when

the stable and unstable invariant curves touch each other, but do not coincide. This means that at least one of the curves must be non-smooth ('fractal torus'). From the figure one can see that both bifurcation lines of smooth and fractal tori-collision meet at the TCT critical point.

It was observed that fractalization of torus and transition to SNA in the forced circle map is possible also in the critical and subcritial domain ($K \leq 1$) [21,22]. This transition can not be associated with the TDT or TCT points because of absence of a quadratic exteremum. The nature of the criticality was revealed in Ref. [12] as linked with the torus fractalization at the intermittency threshold. To describe the phenomenon a model was used

$$x_{n+1} = f(x_n) + b + \varepsilon \cos 2\pi w n, \tag{13}$$

with $f(x)$ defined as

$$f(x) = \begin{cases} x/(1-x), & x \leq 0.75 \\ 9/2x - 3, & x > 0.75 \end{cases} \tag{14}$$

One branch of the mapping is selected in a form of the fractional-linear function, $x/(1-x)$, which appears naturally in analysis of dynamics near the tangent bifurcation associated with intermittency (e.g. [23-26]). The other branch is attached somewhat arbitrarily to ensure presence of the 're-injection mechanism' in the dynamics and to exclude divergence.

Figure 4 shows a chart of dynamical regimes for the model (13). The white area designates chaotic regime with positive Lyapunov exponent Λ. Gray regions correspond to negative Λ. In the bottom gray area attractor is localized and represented by a smooth torus. The upper border of this region is the bifurcation curve of transition to a delocalized attractor via intermittency. The bifurcation consists in collision of smooth stable and unstable tori with their coincidence, and the Lyapunov exponent at the bifurcation is zero. In the right-hand part of the diagram the bifurcation curve separates regimes of torus and SNA. The bifurcation corresponds to a fractal collision of two invariant curves at some exceptional set of points, and the Lyapunov exponent at the bifurcation is negative. These two parts of the bifurcation border are separated by *the critical point of torus fractalization* (TF) located at

$$\varepsilon_{TF} = 2,\ b_{TF} = -0.597515185376121\ldots \tag{15}$$

4. The classic GM critical point

Critical behavior in the circle map associated with break-up of the golden-mean quasiperiodicity (GM critical point) was discovered first by Shenker

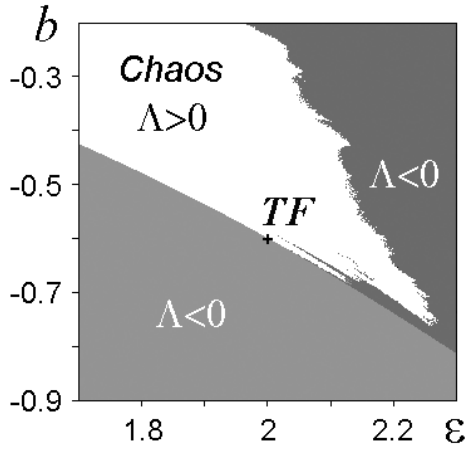

Figure 4. Chart of dynamical regimes for the model (13). The bottom gray area corresponds to localized attractor represented by smooth torus. The upper border is the bifurcation curve of the intermittent transition. In the left part the bifurcation consists in collision of smooth stable and unstable tori with their coincidence, in the right part – to fractal collision at some exceptional set of points. White area designates chaos, and dark gray presumably corresponds to SNA. Sign of the Lyapunov exponent Λ is indicated in all three domains.

[13] and studied in terms of RG analysis by Feigenbaum–Kadanoff–Shenker and Ostlund et al. [7-9]. Although the circle map is one-dimensional, it may be treated in terms of our general scheme, as a particular case of (1). We consider two decoupled maps

$$x_{n+1} = f(x_n), \quad u_{n+1} = u_n + w \pmod 1, \tag{16}$$

with $f(x) = x + r - (K/2\pi)\sin 2\pi x$. The function is independent of the second argument u, so, the GM criticality will correspond to a degenerate fixed point of our functional equation: $g_k(x,u) \equiv G(x)$. In this case Eq.(5) yields

$$G(x) = \alpha^2 G(\alpha^{-1} G(x/\alpha)), \tag{17}$$

the relation known as the Feigenbaum–Kadanoff–Shenker equation. It has been solved numerically (e.g. [7-9, 27-30]), and the function is found in a form of high-precision expansion in powers of x^3. The scaling constant is

$$\alpha = -1.288574553954\ldots \tag{18}$$

Accounting representation of the circle map in the form (16) it is natural to depict the critical attractor in coordinates (u, x) (Fig. 5). Observe that it is represented by a fractal-like curve. Locally, the basic scaling property of this fractal may be deduced from the RG analysis. Indeed, the evolution operators for time intervals increasing as Fibonacci numbers, become

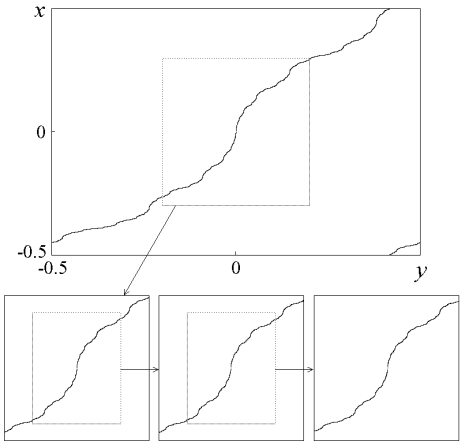

Figure 5. Attractor of the two-dimensional map (16) at the GM critical point (top panel) and illustration of the basic local scaling property: the structure reproduces itself under magnification with factors $a = -1.28857$ and $b = -1.61803$ along the vertical and the horizontal axes, respectively.

identical, up to the scale change. For each next Fibonacci number the variables x and u are rescaled by α and $\beta = -w^{-1}$. As follows, the attractor in coordinates (u, x) must possess self-similarity: increasing resolution by factors α and β along the vertical and the horizontal axes, respectively, one should observe the similar structures (see bottom panels of Fig. 5).

For perturbations of the GM fixed-point, which do not violate the unidirectional nature of the master-slave coupling, the equation (6) accepts the form

$$\delta^2 h(x) = \alpha\delta G'(G(x/\alpha))h(x/\alpha) + \alpha^2 h(\alpha^{-1}G(x/\alpha)). \tag{19}$$

As found (e.g. Refs. [7-9,27-30]), there are two relevant eigenvalues,

$$\delta_1 = -2.8336106559... \text{ and } \delta_2 = \alpha^2 = 1.660424381... \tag{20}$$

These constants are responsible for the scaling properties of the parameter space structure near the GM critical point. However, to demonstrate the scaling we need to define a special local coordinate system near the critical point – the scaling coordinates. (The same will be necessary for other types of criticality, see sections 5-7.) As argued in Refs.[29,30], this is a curvilinear system: one coordinate line goes along the critical line $k = 1$, and another along the curve of constant rotation number. Numerically, a link of new coordinates (C_1, C_2) with the parameters of the original map is expressed as

$$r = r_c + c_1 - 0.01749c_2 - 0.00148c_2^2, \quad k = k_c + c_2. \tag{21}$$

In these equations we account terms up to the second order because of the relation between δ_1 and δ_2: $\delta_2 < \delta_1$ and $\delta_2 < \delta_1^2$, but $\delta_2 > \delta_1^3$ (see Refs. [31,32,11,12] for explanation of the rules for selection of the scaling coordinates). Figure 6 shows a chart of dynamical regimes with Arnold tongues and a sequence of fragments for several steps of magnification in the scaling coordinates. Observe excellent repetition of the two-dimensional arrangement of the tongues at subsequent levels of resolution.

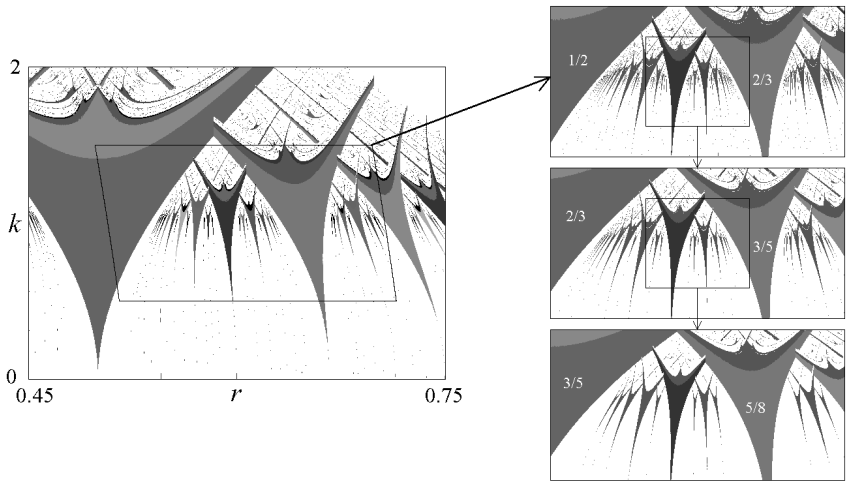

Figure 6. Chart of dynamical regimes on the parameter plane of the sine circle map and a sequence of fragments for several steps of magnification of vicinity of the GM critical point in the scaling coordinates, with factors δ_1 and δ_2 along horizontal and vertical axes, respectively.

5. Critical point TCT

RG analysis of the torus-collision terminal point was developed in Ref. [12]. The critical behavior of this type was found in the forced logistic map (8) and in the forced supercritical circle map (11). Here we prefer to deal with the last one because divergence of iterations is excluded for sure in this case. The equation may be written as

$$\begin{aligned} x_{n+1} &= x_n + r - (K/2\pi)\sin 2\pi x_n + \varepsilon\cos(2\pi u) \ (\mathrm{mod}1), \\ u_{n+1} &= u_n + w \ (\mathrm{mod}1), \end{aligned} \tag{22}$$

and parameter K is supposed to be supercritical and fixed, $K = 2.5$. As mentioned in Sec.2, the TCT point is located at

$$(r,\ \varepsilon)_{TCT} = (0.377866239,\ 0.132566321).$$

In the RG approach, the TCT point is associated with a fixed-point solution of the functional equation (5). This circumstance was checked accurately in the numerical procedure based on iterations of the RG transformation (5). Also the multi-dimensional Newton technique was used to solve the fixed-point equation in respect to the coefficients of polynomial expansion of the universal function in an appropriately chosen domain in the (u, x) plane (see [12] for details). The scaling constant α was found in the course of the computations, so

$$\alpha = 1.7109605\ldots \text{ and } \beta == 1.6180339\ldots \tag{23}$$

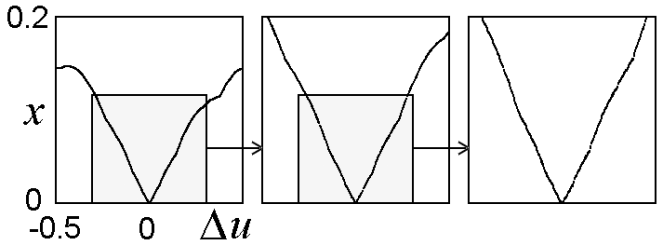

Figure 7. Attractor of the forced circle map at the TCT critical point (the left panel) and illustration of the basic local scaling property: the structure reproduces itself under magnification with factors $\alpha = 1.71096$ and $\beta = -1.61803$ along the vertical and the horizontal axes, respectively.

As seen from Fig. 7, the critical attractor in coordinates (u, x) is represented by a non-smooth fractal-like curve. To observe scaling, we need to select properly the origin of local coordinate system (the 'scaling center'). As found in Ref. [12], it has to be placed at

$$u_c = 0.284109286 \text{ and } x_c = (2\pi)^{-1} \arctan \sqrt{K^2 - 1} = 0.184505060. \tag{24}$$

Now, if we rescale $\Delta x = x - x_c$ and $\Delta u = u - u_c$ by factors α and $\beta = -w^{-1}$, respectively, the dynamical regimes remain of the same kind, but with rescaling of time by factor w^{-1}. The attractor also must be invariant under this transformation. Indeed, the picture inside a selected box in Fig. 7 reproduces itself under subsequent magnifications (with inversion in respect to the phase variable, due to the negative β). This scaling property implies that locally the behavior of the invariant curve obeys $\Delta x \propto |\Delta u|^{\gamma}$ with $\gamma = \log \alpha / \log \beta \cong 1.117$. The power γ is close to one, so visually the curve looks like broken at the point of singularity. Due to ergodicity ensured by irrationality of the frequency ratio, the singularity at the origin implies existence of the same type of singularities over the whole invariant curve, in a dense set of points. Note that $\gamma > 1$. It means that the singularity is

weak: the invariant curve, apparently, remains differentiable, but not twice differentiable.

The next step is analysis of the linearized RG equation and of the corresponding eigenvalue problem (6). Numerical solution of the functional equation with substitution of $g(x,u)$ and constant α associated with the TCT criticality was performed, with approximation of the eigenfunctions via finite power expansions in respect to x and u. As found, two eigenvalues are relevant:

$$\delta_1 = 3.600810\ldots \text{ and } \delta_2 = 1.828329\ldots \tag{25}$$

These are scaling factors determining self-similarity of topography in a vicinity of the TCT point. To demonstrate the scaling property we define scaling coordinates in the parameter plane. Note that $\delta_2 < \delta_1$ and $\delta_2 < \delta_1^2$, but $\delta_2 > \delta_1^3$. So, we account terms up to the second order in the parameter change. As suggested in Ref.[12], it may be chosen as

$$r = r_c + c_1 - 0.3121848c_2 - 2.047c_2^2, \quad \varepsilon = \varepsilon_c + c_2. \tag{26}$$

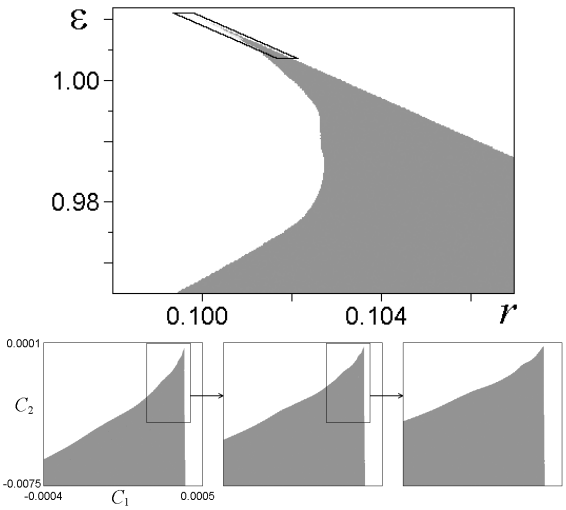

Figure 8. Chart of dynamical regimes on the parameter plane of the quasiperiodically driven supercritical circle map and a sequence of fragments for several steps of magnification of a vicinity of the TCT critical point in the scaling coordinates, with factors δ_1 and δ_2 along horizontal and vertical axes, respectively. Gray area corresponds to localized attractor with negative Lyapunov exponent, and white to chaos.

Figure 8 shows a fragment of the chart of dynamical regimes near the TCT point for the forced circle map. Note similarity of the configurations represented in the scaling coordinates.

6. Critical point TDT

Let us turn now to the RG results for the torus-doubling terminal point [10,33]. The basic illustrative example will be the forced logistic map that may be rewritten as

$$x_{n+1} = \lambda - x_n^2 + \varepsilon \cos 2\pi u_n, \quad u_{n+1} = u_n + w \ (\mathrm{mod}1). \tag{27}$$

As noted in Sec. 2, the TDT point is located at
$(\lambda,\ \varepsilon)_{TDT} = (1.158096856,\ 0.360248020)$.

It was found in Refs.[10,33] that the TDT point is associated with a period-3 cycle of the RG equation (5): $g_1(x,u) \to g_2(x,u) \to g_3(x,u) \to g_1(x,u)$. To find this period-3 solution with high precision a numerical procedure was developed. The result is a representation of functional pair $\{g_1(x,u),\ g_2(x,u)\}$ in a form of polynomial expansions over the arguments x and u (see the table of coefficients in [33]). The rescaling constant is $\alpha = 1.58259341\ldots$

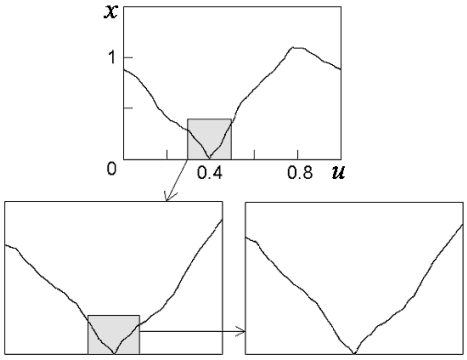

Figure 9. Attractor of the forced logistic map at the TDT critical point and illustration of the basic local scaling property: the structure reproduces itself under magnification with factors $\alpha = 3.96376$ and $\beta = -4.2360$ along the vertical and the horizontal axes, respectively.

In coordinates $(u,\ x)$ the critical attractor looks like a fractal curve (Fig. 9). To observe scaling, the origin of the coordinate system must be placed at the 'scaling center' [10,33]

$$u_c = 0.3952188264 \text{ and } x_c = 0. \tag{28}$$

Due to the period-3 nature of the solution of the RG equation, observation of self-similarity of the critical attractor requires using the scaling factors

$$\alpha^3 = 3.96376647\ldots \text{ and } \beta^3 = -4.23606798\ldots \tag{29}$$

If we rescale x and $\Delta u = u - u_c$ by α^3 and β^3, respectively, the dynamical regimes remain of the same kind, but with characteristic time rescaled by w^{-3}. The curve representing the attractor must be invariant under this transformation, and this is indeed the case, see Fig. 9. The picture inside a selected box reproduces itself under subsequent magnifications. Locally the invariant curve behaves as $x \propto |\Delta u|^\gamma$ with $\gamma = \log\alpha/\log\beta \cong 0.954$. The exponent is close to one, so the curve looks like broken at the point of singularity. Due to ergodicity of the quasiperiodic motion, the singularity at the origin implies presence of the same type of singularities on a dense set of points over the whole invariant curve. As $\gamma < 1$, the curve is not differentiable.

Because of the period-3 nature of the RG equation solution, analysis of the linearized RG equation is more complicated than that for a fixed point. The eigenvalue problem reads

$$\begin{aligned}
\delta^2 h_3(x,u) = {} & \alpha\delta g_1'(g_2(x/\alpha,-uw), w^2u+w)h_2(x/\alpha,-uw) \\
& +\alpha^2 h_1(\alpha^{-1}g_2(x/\alpha,-uw), w^2u+w), \\
\delta^2 h_1(x,u) = {} & \alpha\delta g_2'(g_3(x/\alpha,-uw), w^2u+w)h_3(x/\alpha,-uw) \\
& +\alpha^2 h_2(\alpha^{-1}g_3(x/\alpha,-uw), w^2u+w), \\
\delta^2 h_2(x,u) = {} & \alpha\delta g_3'(g_1(x/\alpha,-uw), w^2u+w)h_1(x/\alpha,-uw) \\
& +\alpha^2 h_3(\alpha^{-1}g_1(x/\alpha,-uw), w^2u+w).
\end{aligned} \tag{30}$$

Numerical solution of this problem with substitution of $g_{1,2,3}(x,u)$ and α associated with the TDT criticality yields two relevant eigenvalues [10,33]:

$$\delta_1 = 10.5029... \text{ and } \delta_2 = 5.1881... \tag{31}$$

To demonstrate scaling property in the parameter plane we need to define appropriate scaling coordinates. In the present case $\delta_2 < \delta_1$ and $\delta_2 > \delta_1^m$ for $m = 2, 3, \ldots$. It means that a linear parameter change is sufficient. According to Refs.[10,33], it may be chosen as

$$\lambda = \lambda_{TDT} + c_2, \quad \varepsilon = \varepsilon_{TDT} - c_1 + 0.3347c_2. \tag{32}$$

Figure 10 shows a chart of dynamical regimes near the TDT in scaling coordinates for several steps of subsequent magnification.

7. Critical point TF

The transition from localized to delocalized attractor in the model map (13) is accompanied by appearance of intermittent regimes. While we are close to the point of bifurcation, the laminar stages of dynamics occupy an overwhelming part of observation time (like in the case of the usual

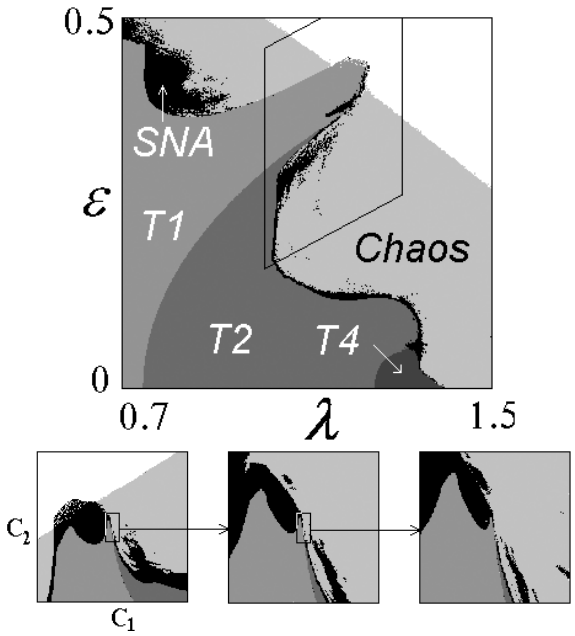

Figure 10. Chart of dynamical regimes on the parameter plane of the quasiperiodically driven logistic map and a sequence of fragments for several steps of magnification of a vicinity of the TDT critical point in the scaling coordinates, with factors δ_1 and δ_2 along horizontal and vertical axes, respectively. Gray area corresponds to localized attractor with negative Lyapunov exponent, and white to chaos.

Pomeau-Manneville intermittency). They correspond to dynamics on the left branch of the map (13). To study details of the transition we may concentrate on the laminar stages and consider a simplified map

$$x_{n+1} = x_n/(1-x_n)+b+\varepsilon\cos(2\pi(nw+u)), \quad u_{n+1} = u_n + w \pmod 1. \quad (33)$$

As explained in Sec.2, the bifurcation border in the plane (ε, b) contains a critical point TF separating situations of smooth and fractal tori collision at $(\varepsilon,\ b)_{TF} = (2,\ -0.597515185)$.

An important note is that due to the fractional-linear nature of the map the functions obtained at subsequent steps of the RG transformation (5) will be fractional-linear too. The same is true for the fixed-point of the RG equation, associated with the TF critical point. It implies that we may search a solution for the fixed-point in a form

$$g(x,u) = (a(u)x + b(u))/(c(u)x + d(u)), \quad (34)$$

where a, b, c, d are some functions of u. Without loss of generality we require them to satisfy additional conditions $a(u)d(u) - b(u)c(u) \equiv 1$ and $c(0) = 1$.

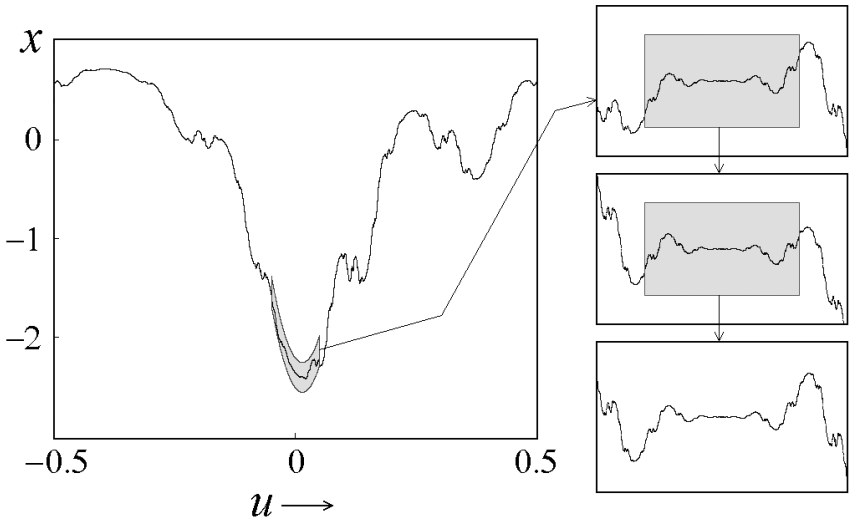

Figure 11. Attractor of the forced fractional-linear map at the TF critical point (the left panel) and illustration of the basic local scaling property: the structure depicted in scaling coordinates reproduces itself under magnification with factors $\alpha = 2.89005$ and $\beta = -1.618034$ along the vertical and the horizontal axes, respectively.

Substituting (34) into (5) we arrive at the fixed-point RG equation in terms of the functions a, b, c, d:

$$\begin{pmatrix} a(u) & b(u) \\ c(u) & d(u) \end{pmatrix} = \begin{pmatrix} a(w^2u+w) & \alpha^2 b(w^2u+w) \\ \alpha^{-2}c(w^2u+w) & d(w^2u+w) \end{pmatrix} \cdot \begin{pmatrix} a(-wu) & \alpha b(-wu) \\ \alpha^{-1}c(-wu) & d(-wu) \end{pmatrix}. \tag{35}$$

The solution was found numerically, and the coefficients of polynomial expansions for $a(u)$, $b(u)$, $c(u)$, $d(u)$ are listed in Ref. [12]. The factor α was also computed, so

$$\alpha = 2.890053525\ldots \text{ and } \beta = -w^{-1} = 1.6180339\ldots \tag{36}$$

These two constants determine scaling properties of the critical attractor on the (x,u)-plane. In fact, the variable x in the RG equation is not the same as in the original map: we need to introduce scaling coordinates in the (x,u)-plane. As found numerically [12], the variable change looks like

$$X \propto x + 2.34719526 + 5.92667u - 210.629u^2, \;\; U = u. \tag{37}$$

Figure 11 illustrates scaling property of the critical atttractor. Observe excellent reproduction of details of the structure in scaling coordinates (X,u).

Numerical solution of the eigenvalue problem (6) for the fractional-linear fixed point reveals two relevant eigenvalues

$$\delta_1 = 3.134272989\ldots \text{ and } \delta_2 = w^{-1} = 1.618033979\ldots \tag{38}$$

They are responsible for scaling properties of the parameter space near the critical point. If we depart from the critical point along the bifurcation curve, the first eigenvector does not contribute; the relevant perturbations are associated with δ_2. If we choose a transversal direction, say, along the axis b, the perturbation of the first kind (δ_1) appears.

In the case under consideration we have $\delta_1 > \delta_2$ and $\delta_1 > \delta_2^2$, but $\delta_1 < \delta_2^3$, so only linear and quadratic terms must be taken into account in the parameter change. The scaling coordinates (C_1, C_2) are linked with parameters of the original map as

$$b = b_{TF} + C_1 - 0.64938C_2 - 0.33692C_2^2, \quad \varepsilon = 2 + C_2. \tag{39}$$

To illustrate scaling associated with the nontrivial constant δ_1 let us consider duration of laminar phases in a course of intermittent dynamics generated by the map (33). In usual Pomeau – Manneville intermittency of type I the average duration of the laminar stages behaves as $\langle t_{\rm lam}\rangle \propto \Delta b^{\nu}$ with $\nu = 0.5$ [23-26]. In presence of the quasiperiodic force the same law is valid in the subcritical region, $\varepsilon < 2$. In the critical case $\varepsilon = 2$ the exponent is distinct. Indeed, as follows from the RG results, to observe increase of a characteristic time scale by factor $\theta = w^{-1} = 1.61803$ we have to decrease a shift of parameter b from the bifurcation threshold by factor $\delta_1 = 3.13427$. As follows, the exponent must be $\nu = \log\theta/\log\delta_1 \cong 0.42123$. Figure 12 shows data of numerical experiments with the fractional-linear map. At each fixed ε in average duration of passage through the "channel" near the formerly existed attractor-repeller pair was computed in dependence on Δ for ensemble of orbits with random initial conditions. Results are plotted in the double logarithmic scale. For particular $\varepsilon = 1.7$ (subcritical) and 2 (critical) the dependencies fit the straight lines of a definite slope, estimated as 0.508 and 0.424, in good agreement with the theory. At subcritical ε slightly less than 2 one can observe a "crossover" phenomenon: the slope changes from the critical to the subcritical one at some intermediate value of Δb.

8. Conclusion

The present paper was devoted to a review of critical situations at the onset of chaotic or strange nonchaotic behavior via quasiperiodicity, more concretely, in the case of the golden-mean ratio of the basic frequencies. We

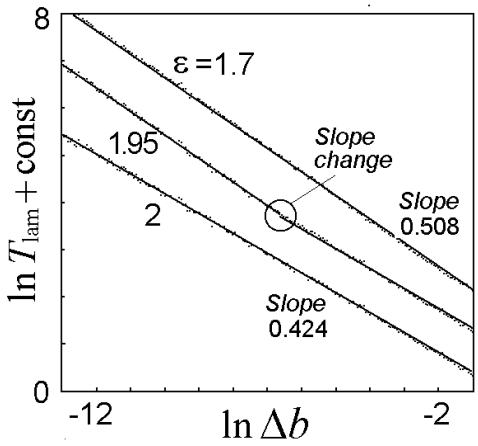

Figure 12. Data of numerical experiments with the fractional-linear map: average duration of passage through the 'channel' versus deflection from the bifurcation threshold for three values of ε in the double logarithmic scale. Observe a 'crossover' phenomenon, the slope change from critical to subcritical value at some intermediate value of Δb for $\varepsilon = 1.95$.

have derived a two-dimensional generalization of the Feigenbaum-Kadanoff-Shenker RG equation and demonstrate that it may be used to treat a number of critical situations – the conventional golden-mean criticality (GM) and the critical behaviors in quasiperiodically driven model maps: torus collision terminal (TCT), torus-doubling terminal (TDT), and torus fractalization at the intermittency threshold (TF). All these critical situations are of obvious interest for a problem of synchronization in nonlinear systems, in the context of study of transitions associated with break-up or other bifurcations of complex generalized synchronous regimes. In perspective, it would be interesting to reveal details and regularities of coexistence and subordination of all the types of critical behavior.

As is common in situations allowing the RG analysis, one can expect that the quantitative regularities intrinsic to our model maps will be valid also in other systems relating to the same universality classes. It would be significant to find these types of behavior in systems of higher dimension, for example, in quasiperiodically driven invertible 2D maps, which could represent Poincare maps of some flow systems. It would be interesting to arrange special experiments on search and observation of the considered types of critical behavior in physical sysyems. Since now, only GM critical behavior was studied experimentally in some details, see e.g. [35,20, 36], and the TDT criticality was observed in a particular quasiperiodically forced electronic system [33,34]).

Acknowledgements

I thank U. Feudel, E. Neumann, A. P. Kuznetsov, A. Pikovsky, and I. Sataev for fruitful collaboration, discussions, and valuable help during a work on different parts of the present research.

This work was supported by RFBR (grants No 00-02-17509 and 03-02-16074) and CRDF (award REC-006).

References

1. A. Pikovsky, M. Rosenblum, and J. Kurths. Synchronization: Universal Concept in Nonlinear Sciences. Cambridge University Press, 2001.
2. C.Grebogi, E.Ott, S.Pelikan and J.A.Yorke. Strange attractors that are not chaotic. Physica **D13**, 1984, 261-268.
3. F.J.Romeiras, A.Bondeson, E.Ott, T.M.Antonsen, and C.Grebogi. Quasiperiodically forced dynamical systems with strange nonchaotic attractors. Physica **D26**, 1987, 277-294.
4. A.S.Pikovsky and U.Feudel. Characterizing strange nonchaotic attractors. Chaos **5**, 1995, 253-260.
5. M.J.Feigenbaum. Quantitative universality for a class of nonlinear transformations. J. Statist. Phys. **19**, 1978, 25-52.
6. M.J.Feigenbaum. The universal metric properties of nonlinear transformations, J. Statist. Phys. **21**, 1979, 669-706.
7. M.J.Feigenbaum, L.P.Kadanoff, S.J.Shenker. Quasiperiodicity in dissipative systems. A renormalization group analysis. Physica **D5**, 1982, 370-386.
8. D.Rand, S.Ostlund, J.Sethna, and E.D.Siggia. A universal transition from quasiperiodicity to chaos in dissipative systems. Phys. Rev. Lett. **49**, 1082, 132-135.
9. S.Ostlund, D.Rand, J.Sethna, and E.D.Siggia. Universal properties of the transition from quasi-periodicity to chaos in dissipative systems. Physica **D8**, 1983, 303-342.
10. S.P.Kunetsov, U.Feudel and A.S.Pikovsky. Renormalization group for scaling at the torus-doubling terminal point. Phys.Rev.**E57**, 1998, 1585-1590.
11. S.P.Kuznetsov, E.Neumann, A.Pikovsky, I.R.Sataev. Critical point of tori-collision in quasiperiodically forced systems. Phys.Rev. **E62**, 2000, No 2, 1995-2007.
12. S.P.Kuznetsov. Torus fractalization and intermittency. Phys.Rev. **E65**, 2002, 066209.
13. S. J. Shenker. Scaling behavior in a map of a circle onto itself. Empirical results. Physica **D5**, 1982, 405-411.
14. K.Kaneko. Doubling of torus. Progr.Theor.Phys., **69**, 1983, 1806-1810.
15. S.P.Kuznetsov. Effect of a periodic external perturbation on a system which exhibits an order-chaos transition through period-doubling bifurcations. JETP Lett. **39**, 1984, No 3, 133-136.
16. K.Kaneko. Oscillation and doubling of torus. Progr.Theor.Phys. **72**, No 2, 1984, 202-215.
17. A.Arneodo. Scaling for a periodic forcing of a period-doubling system. Phys.Rev.Lett. **53**, 1984, 1240-1243.
18. S.P.Kuznetsov, A.S.Pikovsky. Renormalization group for the response function and spectrum of the period-doubling system. Phys.Lett. **A140**, 1989, 166-172.
19. A.Arneodo, P.H.Collet, E.A.Spiegel. Cascade of period doublings of tori. Phys.Lett. **A94**, 1983, 1-4.

20. V.S.Anishchenko. Dynamical Chaos - Models and Experiments. Appearance, Routes and Structure of Chaos in Simple Dynamical Systems (World Scientific, Singapore, 1995).
21. U.Feudel, A.S.Pikovsky, and J.Kurths. Strange non-chaotic attractor in a quasiperiodically forced circle map, Physica **D88**, 1995, 176-186.
22. H.Osinga, J.Wiersig, P.Glendinning and U.Feudel. Multistability and nonsmooth bifurcations in the quasiperiodically forced circle map. Int. J. Of Bifurcation and Chaos, **11**, 2001, 3085-3107.
23. Y.Pomeau, P.Manneville. Intermittent transition to turbulence in dissipative dynamical systems. Commun. Math. Phys. **74**, 1980, 189-197.
24. B.Hu, J.Rudnik. Exact solution of the Feigenbaum renormalization group equations for intermittency. Phys.Rev.Lett., **48**, 1982, 1645-1648.
25. J.E.Hirsch, B.A.Huberman, and D.J.Scalapino. Theory of intermittency. Phys. Rev. **A25**, 519-532 (1982).
26. F.Argoul and A.Arneodo. Scaling for periodic forcing at the onset of intermittency. J. Phys. Lett. (Paris) **46**, L901 (1985).
27. K.M.Briggs, T.W.Dixon, G.Szekeres. Analytic solution of the Cvitanovic-Feigenbaum and Feigenbaum-Kadanoff-Shenker equations. Int.J.of Bifurcation and Chaos, **8**, 1998, 347-357.
28. T.W.Dixon, T.Gherghetta, B.G.Kenny. Universality in the quasiperiodic route to chaos. CHAOS, **6**, 1996, 32-42.
29. N.Yu.Ivankov, S.P.Kuznetsov. Complex periodic orbits, renormalization and scaling for quasiperiodic golden-mean transition to chaos. Phys.Rev. **E63**, 2001, 046210.
30. S.P.Kuznetsov. Dynamical Chaos. Moscow, Fizmatlit, 2001, 296p. (In Russian.)
31. A.P.Kuznetsov, S.P.Kuznetsov, I.R.Sataev. A variety of period-doubling universality classes in multi-parameter analysis of transition to chaos. Physica **D109**, 1997, 91-112.
32. A.P.Kuznetsov, S.P.Kuznetsov, I.R.Sataev. Three-parameter scaling for one-dimensional maps. Phys.Lett **A189**, 1994, 367-373.
33. B.P.Bezruchko, S.P.Kuznetsov, A.S.Pikovsky, Ye.P.Seleznev, U.Feudel. On dynamics of nonlinear systems under external quasi-periodic force near the terminal point of the torus doubling bifurcation curve. Applied Nonlinear Dynamics, **5**, 1997, No 6, 3-20. (In Russian.) See also http://www.sgtnd.tserv.ru/eng/index.htm.
34. B.P.Bezruchko, S.P.Kuznetsov, Ye.P.Seleznev. Experimental observation of dynamics near the torus-doubling terminal critical point. Phys.Rev. **E62**, 2000, No 6, 7828-7830.
35. J.A.Glazier, G.Gunaratne, A.Libchaber. $F(\alpha)$ curves – Experimental results. Phys.Rev. **A37**, 1988, 523-530.
36. D.Barkley, A.Cumming. Thermodynamics of the quasi-periodic parameter set at the borderline of chaos – Experimental results. Phys.Rev.Lett., **64**, 1990, 327-331.